Gravitational waves from relativistic rotational core collapse in axisymmetry

H Dimmelmeier, J A Font†, and E Müller

Max-Planck-Institut für Astrophysik, Karl-Schwarzschild-Str. 1,
D-85740 Garching, Germany.

Abstract. We present results from simulations of axisymmetric relativistic rotational core collapse. The main objective of our investigation is to compute the waveforms of gravitational radiation emitted in such events, extending previous Newtonian simulations to relativity. The general relativistic hydrodynamic equations are formulated in flux-conservative form and solved using a high-resolution shock-capturing scheme. The Einstein equations are solved assuming a conformally flat 3-metric and the quadrupole formula is used to extract waveforms of the gravitational radiation emitted during the collapse. A comparison of our results with those of Newtonian simulations shows that gravitational wave amplitudes agree within 30%. Surprisingly, in some cases, relativistic effects actually diminish the amplitude of the gravitational wave signal. We further find that the parameter range of models suffering multiple coherent bounces due to centrifugal forces is considerably smaller than in Newtonian simulations.

Submitted to: *Class. Quantum Grav.*

PACS numbers: 04.25.Dm, 04.25.Nx, 04.30.Db, 95.30.Sf, 97.60.Bw

1. Introduction

Numerical studies of supernova core collapse are a rich and complex field of astrophysics, involving very different physical aspects [1]. In the advent of experimental gravitational wave astronomy [2], the predictions from astrophysical simulations of this problem are becoming very important. In particular, the waveforms of gravitational radiation emitted during the collapse will be of use for data analysis in gravitational wave detectors [3]. However, theoretical predictions of the gravitational wave signal from rotational core collapse are still hampered by two major reasons: Firstly, the rotational state of the core prior to its gravitational collapse is not known due to the lack of multi-dimensional evolutionary calculations of rotating stars. Thus, predictions from rotational core collapse must rely upon extensive parameter studies. Secondly, reliable collapse simulations require a relativistic treatment of the dynamics, the incorporation of a realistic equation of state (EoS) and neutrino transport. Due to such complexities, all previous studies have either neglected or approximated one or all of these requirements.

† Present address: Departamento de Astronomia y Astrofisica, Universidad de Valencia, 46100 Burjassot, Spain.

Previous studies of axisymmetric rotational core collapse to a neutron star, which either investigated a few Newtonian models with a realistic EoS and simplified neutrino treatment [4], or a large set of Newtonian models with a simplified EoS and no neutrino transport [5], predict gravitational wave signals which yield a maximum dimensionless strain $h \sim 10^{-23} \cdot (10 \text{ Mpc}/R)$ for a source at a distance R. The total emitted gravitational wave energy was found to be $\sim 10^{-6} M_\odot c^2$, where $M_\odot = 1.99 \times 10^{33}$ g is the sun's mass, and c is the speed of light. Thus, the collapse dynamics is not influenced by the gravitational radiation backreaction. The present work extends the axisymmetric Newtonian core collapse simulations of [5] to relativity to improve the reliability of the prediction of the gravitational wave signal from rotational core collapse.

2. Physical model

In order to be able to examine a large set of collapse conditions we approximate the collapsing core by a rotating polytrope and use a simplified analytic EoS [6]. We neglect all transport effects but include relativistic dynamics in a time-dependent spacetime. The pressure P consists of a polytropic part and a thermal part, $P(\rho, \epsilon) = P_\mathrm{p} + P_\mathrm{th} = K\rho^{\gamma_\mathrm{p}} + \rho\epsilon_\mathrm{th}(\gamma_\mathrm{th} - 1)$, where ρ is the rest-mass density, and $\epsilon = \epsilon_\mathrm{p} + \epsilon_\mathrm{th}$ is the specific internal energy which is the sum of a polytropic and a thermal contribution. The polytropic constant K and the polytropic index γ_p change discontinuously at nuclear matter density, $\rho_\mathrm{nuc} = 2.0 \times 10^{14}$ g cm^{-3}, but are independent of ρ elsewhere. P_th mimics the thermal pressure in the matter heated by the shock. In all models we set $\gamma_\mathrm{th} = 1.5$, corresponding to a mixture of relativistic and nonrelativistic gas.

The initial configurations are rotating relativistic stellar cores in equilibrium computed by means of Hachisu's self-consistent field method [7]. All initial models are 4/3-polytropes, $P = K\rho^{4/3}$, with a central density of 1.0×10^{10} g cm^{-3}. They rotate according to the differential rotation law specified in [7], in which a parameter A determines the angular momentum distribution. For large values of A the configurations rotate almost rigidly; small values of A correspond to strongly differential rotation. The initial model is further specified by the ratio of the rotational energy to the modulus of the gravitational potential energy, $\beta = E_\mathrm{rot}/|E_\mathrm{pot}|$. The collapse is initiated by reducing γ_p from $4/3$ to some prescribed value in the range $[1.28, 1.325]$. In all simulations we assume axial and equatorial plane symmetry.

3. Equations and numerical methods

The hydrodynamic evolution of a relativistic fluid in a spacetime with a metric $g_{\mu\nu}$ is governed by the local conservation laws of the current density $J^\mu = \rho u^\mu$ and the (perfect fluid) stress-energy $T^{\mu\nu} = \rho h u^\mu u^\nu + P g^{\mu\nu}$, where u^μ is the 4-velocity and $h = 1 + \epsilon + P/\rho$ is the specific enthalpy. We define a set of conserved variables $D = \rho W$ (rest-mass density), $S_i = \rho h W^2 v_i$ (momentum density), and $E = \rho h W^2 - P$ (total energy density) in terms of the primitive variables (ρ, v_i, ϵ). Here W is the Lorentz factor, and v_i is the 3-velocity. Then the hydrodynamic equations can be written as a first-order flux-conservative hyperbolic system of conservation laws [8].

The time-dependent metric is evolved using the 3+1 splitting of spacetime. In this formalism the Einstein equations are written as a system of evolution and constraint equations for the 3-metric γ_{ij} and the extrinsic curvature K_{ij} (ADM equations). Unfortunately, achieving long-term stable evolution using the 3+1 system (or improved reformulations) is still an open issue. Therefore, following [9]‡, we approximate the spacetime geometry by assuming that the 3-metric is conformally flat, i.e. $\gamma_{ij} = \phi^4 \hat{\gamma}_{ij}$ where ϕ is a coordinate-dependent conformal factor, and $\hat{\gamma}_{ij}$ is the flat 3-metric (conformal flatness condition – CFC)§. In this approximation, the Einstein equations transform into a system of 5 coupled nonlinear elliptic equations for the conformal factor ϕ, the lapse function $\alpha = 1/\sqrt{-g^{00}}$, and the shift vector $\beta^i = \alpha^2 g^{0i}$ [9]. At least in the case of rotational core collapse investigated in this work, this coupled system of hydrodynamic and metric equations exhibits long term numerical stability.

In order to exploit the hyperbolic and conservative character of the hydrodynamic equations, our numerical code uses a Godunov-type flux-conservative finite volume scheme based on the solution of approximate Riemann problems (see e.g. [13]). On each time slice, the hydrodynamic data are represented by cell averages of the conserved quantities D, S_i and E. These are propagated to the next time level by a conservative Runge–Kutta algorithm, which involves the numerical fluxes and sources. The metric equations for ϕ, α, and β^i are solved by a Newton–Raphson iteration scheme. In each iteration, we solve a linear system of equations involving the (sparse) Jacobi matrix of the discretized equations. To pin down the effects of general relativity on rotational core collapse, we have compared relativistic and Newtonian simulations for a large set of initial models. The simulations have been performed in spherical coordinates using a logarithmic radial grid with 200 zones and an equidistant angular grid with 30 zones.

As the off-diagonal elements of γ_{ij} are set to zero in the CFC approach, the gravitational wave content of the spacetime is eliminated. Therefore, to compute the gravitational wave signal we use a form of the Einstein quadrupole formula (avoiding explicit time derivatives [5]) in a post-processing step.

4. Results

For testing the accuracy of the numerical schemes, we have performed a comprehensive number of tests. We have demonstrated that the code is able to keep rotating neutron star models with different rotation rates and profiles in equilibrium over many rotation periods. Furthermore, when applying our Eulerian code to core collapse in spherical symmetry, we find good agreement with results obtained from a May–White-type Lagrangian code with artificial viscosity [14].

The accuracy of the CFC approach has been considered in [15], finding remarkably good results for rapidly rotating relativistic stars in equilibrium. The accuracy degrades for extremely relativistic nonspherical configurations, e.g. rigidly rotating infinitesimally thin disks of dust [16]. Tests performed by us demonstrate that for rapidly rotating equilibrium configurations, the CFC metric approximates the exact ADM metric very well even for relativistic and strongly deformed spacetimes. We have additionally estimated the accuracy of the CFC approximation by re-inserting the conformally flat metric into the ADM metric equations (for a brief discussion, see [17]). These estimates will be elaborated in more detail in an upcoming paper.

Here we present the results from three representative models (see Table 1). The time-evolution of the central density ρ_c and of the gravitational wave signal amplitude A_{20}^{E2} are plotted in the left and right panels of figure 1, respectively.

‡ See [10, 11] for corrections.

§ We note that a similar approach to simulate rotational core collapse has recently been proposed in [12].

Table 1. Model parameters. Subscripts R and N denote relativistic and Newtonian simulations, respectively. Note that model B never reaches $\rho_{\rm nuc}$.

Model	A (10^8 cm)	$\beta_{\rm R}$ (%)	$\beta_{\rm N}$ (%)	$\gamma_{\rm p}$ ($\rho \leq \rho_{\rm nuc}$)	$\gamma_{\rm p}$ ($\rho > \rho_{\rm nuc}$)
A	0.5	0.472	0.476	1.300	5/3
B	1.0	1.817	1.807	1.325	—
C	0.5	0.472	0.476	1.325	2.5

The signal amplitude $A^{\rm E2}_{20}$ relates to the quadrupole radiation field $h^{\rm TT}_{\theta\theta}$ as $h^{\rm TT}_{\theta\theta} = 1/8\sqrt{15/\pi}\sin^2\theta \cdot A^{\rm E2}_{20}/R$, where θ is the angle between the line of sight and the rotation axis of the source, and R is the distance to the source [5]. Thus, the maximum strain is given as $h \equiv h^{\rm TT}_{\theta\theta}(\theta = \pi/2) = 8.85 \times 10^{-24} \cdot (A^{\rm E2}_{20}/1000 \text{ cm}) \cdot (10 \text{ Mpc}/R)$.

Model A is a strongly differentially rotating core which contracts rapidly (time of bounce $t_{\rm b} = 38$ ms) due to a low adiabatic index $\gamma_{\rm p}$. The bounce occurs at a central density well beyond nuclear matter density ($\rho_{\rm c}(t_{\rm b}) = 9.3 \times 10^{14}$ g cm^{-3}) because the supranuclear EoS was chosen to be extremely soft. After bounce the rotating core oscillates with a superposition of various radial and axisymmetric modes (ring-down). The oscillation frequencies of the core are higher in relativistic gravity due to the higher densities in the central regions. However, although the maximum central density in relativistic gravity is almost 50% higher than in the Newtonian case, the associated gravitational wave amplitude of the relativistic model is nevertheless considerably lower. This surprising result can be explained by noting that in the quadrupole formula, the gravitational wave amplitude is determined by the second time derivative of the total quadrupole moment of the core, which involves a volume integral where the integrand is proportional to ρr^4. Thus, higher densities in the central regions of the core due to relativistic effects do not necessarily imply a stronger signal. Instead, one must take into account the entire density distribution. We find that in model A the deeper relativistic gravitational potential results in a more compact density distribution in the interior regions of the core, whereas the density in the Newtonian simulation is higher for radii $\gtrsim 5$ km (density crossing) [17]. This gives rise to a larger quadrupole moment in the Newtonian simulation, and hence to the observed larger gravitational wave amplitude.

Model B is initially an almost rigid rotator, which bounces later ($t_{\rm b} = 98$ ms) than model A due to its larger subnuclear adiabatic index. The collapse is stopped at subnuclear densities ($\rho_c(t_{\rm b}) = 3.8 \times 10^{13}$ g cm^{-3}) by the rapid spin-up of the core due to angular momentum conservation. After bounce the core first expands, then begins to collapse once more and rebounces again. The phenomenon of homologous multiple bounces [4] was observed in the Newtonian simulations of [5] for strongly differentially rotating configurations with a sufficiently large initial value of β and a subnuclear $\gamma_{\rm p}$ close to 4/3. In model B the relativistic effects cause the bounce to occur at much higher densities, and the interval between the multiple bounces is also shortened. Therefore, in this case the gravitational wave amplitude of the relativistic model is actually somewhat larger than in the Newtonian one.

Compared to the Newtonian simulations in [5], we find that general relativistic models show distinct multiple bounces only for a few extremely rapidly and differentially rotating initial models. In our relativistic simulations, the central density of most of the models, which bounce at subnuclear densities in Newtonian gravity,

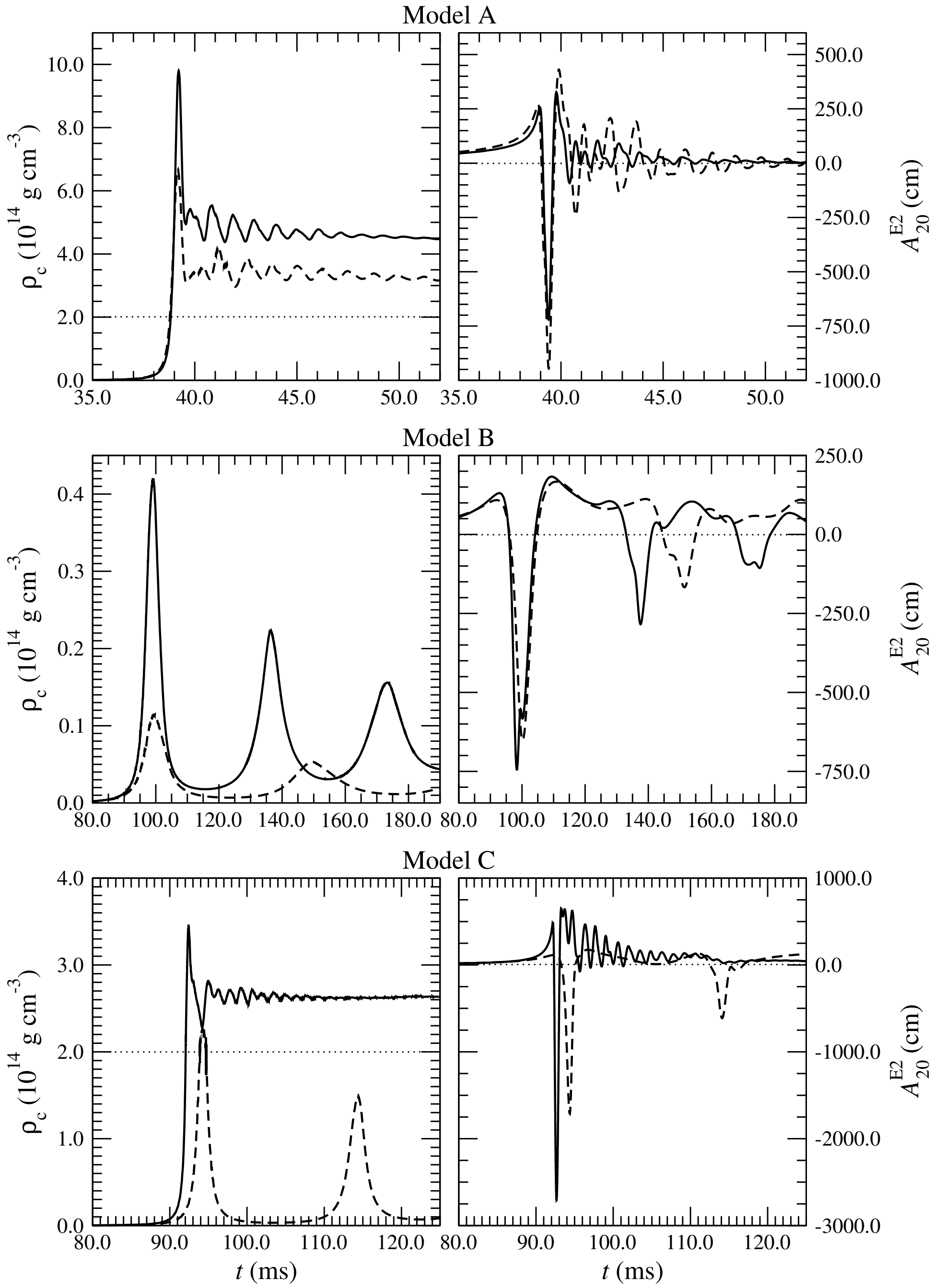

Figure 1. Time-evolution of the central density ρ_c (left panels) and of the gravitational wave signal amplitude A_{20}^{E2} (right panels) for model A (top), B (middle) and C (bottom); relativistic runs are denoted by solid lines, Newtonian runs by dashed lines. Note the transition in model C from multiple bounce collapse in Newtonian gravity to regular collapse in relativistic gravity. The horizontal dotted lines in the density plots mark nuclear matter density.

exceeds nuclear matter density, and the stiffening of the EoS destroys the coherence of the bounce. In model C, which exhibits such a behavior, the evolution of the central density clearly reflects this change of collapse type due to relativistic effects. As a consequence, the corresponding waveforms differ significantly: In the Newtonian simulation, a characteristic multiple bounce signal with several distinct peaks can be observed, whereas the waveform of the relativistic simulation shows a structure with typical regular collapse features like a single burst and a subsequent ring-down signal. This change of collapse types and its manifestation in the gravitational wave signal may have important consequences on the possibility to make inferences from an observed signal to the parameter space of the collapse event.

As our relativistic simulations yield signal amplitudes similar to Newtonian models (despite a possible qualitative change of the waveform), the prospects for detection of rotational core collapse events are also similar. Therefore the predicted signal strength of Galactic events lies within the sensitivity range of the upcoming gravitational wave interferometers [2]. However, extragalactic events seem to be too weak for current detector sensitivities. To further improve the waveforms, 3-dimensional effects and advanced microphysics have to be taken into account. We end by pointing out that we will make a catalogue of the signal waveforms of all investigated models publicly available in the near future.

Acknowledgments

It is a pleasure to thank Y. Eriguchi, J. Mª Ibáñez, and G. Schäfer for suggestions and helpful discussions. The calculations were carried out at the Rechenzentrum Garching and MPI für Astrophysik, Garching.

References

[1] Müller E 1998 *Computational methods for astrophysical fluid flow. Saas-Fee Advanced Course 27* ed O Steiner and A Gautschy (Berlin: Springer) p 343
[2] Thorne K S 1997 *Rev. Mod. Astron.* **10** 1 (Thorne K S 1997 *Preprint* gr-qc/9704042)
[3] Pradier T *et al* 2000 *Preprint* gr-qc/0010037
[4] Mönchmeyer R *et al* 1991 *Astron. Astrophys.* **246** 417
[5] Zwerger T and Müller E 1997 *Astron. Astrophys.* **320** 209
[6] Janka H-T, Zwerger T and Mönchmeyer R 1993 *Astron. Astrophys.* **268** 360
[7] Komatsu H, Eriguchi Y and Hachisu I 1989 *Mon. Not. R. Astron. Soc.* **237** 355
[8] Banyuls F *et al* 1997 *Astrophys. J.* **476** 221
[9] Wilson J R, Mathews G J and Marronetti P 1996 *Phys. Rev.* D **54** 1317 (Wilson J R, Mathews G J and Marronetti P 1996 *Preprint* gr-qc/9601017)
[10] Flanagan É É 1999 *Phys. Rev. Lett.* **82** 1354 (Flanagan É É 1998 *Preprint* astro-ph/9811132)
[11] Mathews G J and Wilson J R 2000 *Phys. Rev.* D **61** 127304 (Mathews G J and Wilson J R 1999 *Preprint* gr-qc/9911047)
[12] Cardall C Y, Mezzacappa A and Liebendörfer M 2001 *Preprint* astro-ph/0106105
[13] Font J A 2000 *Liv. Rev. Rel.* 2000-2
[14] May M M and White R H 1966 *Phys. Rev.* **141** 1232
[15] Cook G, Shapiro S L and Teukolsky S A 1996 *Phys. Rev.* D **53** 5533 (Cook G, Shapiro S L and Teukolsky S A 1995 *Preprint* gr-qc/9512009)
[16] Kley W and Schäfer G 1999 *Phys. Rev.* D **60** 027501 (Kley W and Schäfer G 1998 *Preprint* gr-qc/9812068)
[17] Dimmelmeier H, Font J A and Müller E 2001 *Astrophys. J. Lett.* **560** L163 (Dimmelmeier H, Font J A and Müller E 2001 *Preprint* astro-ph/0103088)